Draft version February 1, 2008
Preprint typeset using LaTeX style emulateapj v. 10/09/06

arXiv:0706.0864v1 [astro-ph] 6 Jun 2007

BONDI ACCRETION IN THE EARLY UNIVERSE

Massimo Ricotti
Department of Astronomy, University of Maryland, College Park, MD 20742, USA

Draft version February 1, 2008

ABSTRACT

This paper presents a study of quasi-steady spherical accretion in the early Universe, before the formation of the first stars and galaxies. The main motivation is to derive the basic formulas that will be used in a companion paper to calculate the accretion luminosity of primordial black holes and their effect on the cosmic ionization history.

The following cosmological effects are investigated: the coupling of the gas to the CMB photon fluid (*i.e.*, Compton drag), Hubble expansion, and the growth of the dark matter halo seeded by the gravitational potential of the central point mass. The gas equations of motion are solved assuming either a polytropic or an isothermal equation of state. We consider the cases in which the accreting object is a point mass or a spherical dark matter halo with power-law density profile, as predicted by the theory of "secondary infall". Analytical solutions for the sonic radius and fitting formulas for the accretion rate are provided.

Different accretion regimes exist depending on the mass of the accreting object. If the black hole mass is smaller than $\sim 50-100$ M$_\odot$, gas accretion is unaffected by Compton drag. A point mass and an extended dark halo of equal mass accrete at the same rate if $M \gtrsim 5000$ M$_\odot$, while smaller mass dark halos accrete less efficiently than the equivalent point mass. For masses $M \gtrsim 3\times 10^4$ M$_\odot$, the viscous term due to the Hubble expansion becomes important, and the assumption of quasi-steady flow fails. Hence, the steady Bondi solutions transition to the time-dependent self-similar solutions for "cold cosmological infall".

Subject headings:

1. INTRODUCTION

The gravitational collapse of relativistic matter during the early evolution of the universe is thought to produce primordial black holes (PBH). Moderately nonlinear inhomogeneities that become gravitationally unstable after entering the particle horizon have a density and radius that is very close to the black hole regime. It is easy to show that the Jeans length and the Schwarzschild radius of a black hole with mean density close to the cosmic value both approach the particle horizon radius as the effective sound speed of the gas approaches the speed of light. Hence, small density perturbations with $\delta\rho/\rho \sim 0.1-1$ are unstable and collapse into PBHs with a mass that roughly equals the mass within the particle horizon at the redshift of their formation (Hawking 1971; Carr & Hawking 1974; Musco et al. 2005; Harada & Carr 2005).

Many physical processes may produce the necessary level of inhomogeneity for significant PBH formation. In most models PBHs are produced during phase transitions of the equation of state and, depending on the time of their formation, may have masses that range between the Planck mass to 10^5 M$_\odot$. Although the probability of PBH formation is finite, it may be so small to be of little or any cosmological interest. PBHs with mass $< 10^{15}$ g are thought to evaporate emitting Hawking radiation on time scales shorter than the age of the Universe. The radiation or particles they emit would make them detectable. Thus observational constraints on the abundance of evaporating PBHs are rather stringent. The upper limit on the density parameter of PBHs with masses $1g < M_{PBH} < 10^{15}$ g is $\beta(M) \sim 10^{-20} - 10^{-22}$ at the redshift of formation (*e.g.* Carr 2003). On the other hand, the existence of non-evaporating PBHs with mass $> 10^{15}$ g is very poorly constrained. It is conceivable that non-evaporating PBHs constitute all or a substantial fraction of the dark matter in the Universe. The existence of PBHs with $M \sim 0.1-1$ M$_\odot$ is of particular interest because the MACHO collaboration has detected compact objects in this mass range in the Galactic halo, constituting about 20% of the dark matter (Alcock et al. 2000), although this claim is weakened by recent results (*e.g.*, Hamadache et al. 2006). PBHs of about 1 M$_\odot$ are also of special interest theoretically because they may have formed copiously during the quark-hadron phase transition due to a temporary softening of the cosmic equation of state (Jedamzik 1997).

The main motivation for the calculations presented this work is to provide the basic formulas for the accretion rate onto PBHs that, typically, are thought to have masses smaller than 10^5 M$_\odot$. We will show that in this mass range the cosmological spherical accretion solutions are described by the steady equations (*i.e.*, Bondi solutions) while for more massive black holes the accretion equations are time-dependent and the solutions self-similar (*i.e.*, secondary infall solutions).

These formulas will be the foundation for further calculations presented in a companion paper (Ricotti et al. 2006, hereafter, Paper II) aimed to understand whether the interaction between an, as yet undetected, population of non-evaporating PBHs and the rest of the matter in the Universe may produce observable signatures. Thus, in this paper we will only focus on the mathematical aspect of the spherical accretion problem (*i.e.*, for the

Electronic address: ricotti@astro.umd.edu

mass range we are interested in, the solution of the steady "Bondi" problem) without a discussion on the physics of the early universe, feedback effects and other complications. Nevertheless, in the remaining of this introduction we provide some additional background discussion to put the mathematical problem into context.

PBHs can accrete gas and dark matter from a nearly uniform medium (Carr 1981; Miller & Ostriker 2001; Mack et al. 2006) well before the collapse of the first nonlinear structures (stars and galaxies). Since the density inhomogeneities of the gas and dark matter decrease with increasing redshift, we expect the angular momentum of the accreted material (gas and dark matter) to be small and hence, the accretion flow to become increasingly spherical. At redshifts greater than $z \sim 100$, CMB photons are strongly coupled to the gas because of Compton scattering with the residual electrons left over after the epoch of recombination ($x_e \simeq 10^{-4}$). The gas behaves as a viscous fluid and the accretion onto PBHs can be substantially reduced. The photon viscosity may also be important in removing angular momentum from the gas (*e.g.*, Loeb 1993). We will show that the Hubble expansion also acts as a viscous term that tends to reduce the accretion rate, independent of the ionization fraction of the gas. Finally, if massive PBHs do not constitute the bulk of dark matter, their gravitational potential seeds the formation of a dark halo that is expected to grow over time becoming ~ 100 times more massive than the PBH in its center (Mack et al. 2006).

The gas accretion onto PBHs produces ionizing radiation and an X-ray background that may be sufficiently large to heat the cosmic gas and keep it partially ionized after recombination. Thus, PBHs may imprint signatures on CMBR which are incompatible with observations by WMAP3 (Spergel et al. 2006) and such observations can be used to constrain PBH masses and abundances. Several ingredients need to be considered when modeling ionization by accreting PBHs, including their proper motion and feedback effects. The X-rays emitted by accreting PBHs, for example, increase the temperature and fractional ionization of the gas and are able to reduce the accretion rate. Thus the global accretion rate onto PBHs and the ionization state of the cosmic gas are coupled and need to be calculated self-consistently. Such calculations will be presented in a companion paper (Paper II).

The present study focuses on the derivation of the basic analytical relationships for the gas accretion rate as a function of redshift, temperature, density and ionization fraction of the gas. We find solutions for the spherical accretion problem including the following cosmological effects: i) the effect of the viscous terms due to Compton drag and Hubble expansion; ii) we consider both the case of an isolated PBH and the case in which the PBH is "clothed" by a dark matter halo with power-law density profile. We discuss the relationships between the steady Bondi type solutions and the time-dependent-self-similar solutions of secondary infall. Analytical expressions for the accretion rate as a function of the "viscosity parameter" are provided for either a "naked" or "clothed" PBH. We also consider the different cases of isothermal equation of state or polytropic equation of state with index γ for the gas.

Umemura & Fukue (1994) have previously investigated the effect of radiation drag on spherical accretion considering three cases for the gravitational potential: a central point mass, a dark halo with constant potential and a self-gravitating gas sphere. Their work is similar to the present work for the case of accretion onto a point mass. Our work differs from the previous ones in that it addresses the growth of a dark matter halo around PBHs, it discusses the validity of the Bondi accretion regime and the transition to time-dependent solutions. Finally, and most importantly, we derive analytic expressions for the accretion eigenvalues, which are a key ingredient to model the cosmic ionization by PBHs presented in Paper II. Tsuribe et al. (1995) has also investigated a spherically symmetric accretion flow with an external radiation drag onto black holes but for masses that are larger ($> 10^{4-5}$ M$_\odot$) than the ones discussed in this paper. We will show in § 2.1 that in this mass range the steady-state assumption that defines the "Bondi problem" fails and the solutions transition to a class of time-dependent self-similar solutions.

Another interesting mechanism that may lead to the formation in the early universe of massive black holes has been proposed by Loeb (1993); Umemura et al. (1993). These works discuss in detail the effect of CMBR in the accretion process during a quasi-spherical collapse of a self-gravitating gas clouds and the consequent formation of massive black hole in the early universe, after recombination. In this scenario the removal of angular momentum due to Compton drag in collapsing rare density perturbations at redshift $z \sim 400 - 1000$ leads to the formation of massive black holes with masses $M \gtrsim 10^5$ M$_\odot$. Radiation feedback effects associated with the accretion process are also considered. These works differ from the present one in several ways. They focus on the formation of black holes rather than accretion onto a pre-existing black holes and the typical masses of the black holes formed by this process are much more massive than the ones considered in the present study. The accretion is not steady and no Bondi solution exists. Although the black holes formed in this scenario should be very rare, Sasaki & Umemura (1996) have estimated that accretion onto such black holes would produce enough radiation to reionize the universe by $z \sim 150$.

Several authors have investigated the effect that Compton drag and Compton heating has on gas accretion in many different contexts (*e.g.*, Fukue & Umemura 1994; Mineshige et al. 1998; Ciotti et al. 2004; Park & Ostriker 2007). Recently, Wang et al. (2006) presented a discussion of feedback in different accretion regimes, including a Bondi sphere in the case of a black hole accretion at high redshift. They point out that Compton heating can rapidly halt supercritical accretion onto remnant black holes of 10^3 M$_odot$ from Population III stars. Such feedback would prevent seed black holes to grow to masses typical of supermassive black holes on timescale shorter than a Gyr. Thus, they conclude that accretion onto seed black holes from population III stars is not a viable mechanism to explain the existence of quasars at redshift $z \sim 6$. In the present paper the accretion onto PBHs is highly subcritical and Compton heating is unlikely important. However, feedback processes and other physical processes will be addressed in detail in Paper II.

The organization of this paper is as follows. In § 2 we introduce the basic equations for accretion around a point mass in comoving coordinates. In § 3 we solve numerically the accretion equations and provide analytical fits for the accretion eigenvalues. In § 4 we repeat the calculations assuming the gravitational potential of a dark halo with power-law density profile. A summary and discussion is presented in § 5.

2. BASIC EQUATIONS

At high redshift, repeated Compton scattering between free electrons and CMB photons - assumed here to be homogeneous and isotropic - act on the proper velocity of the gas, v, as a viscous term. The forces exerted by the CMB photons are opposed to the motion of the fluid element with respect to the photons' rest frame, producing a mean restoring acceleration (Peebles 1980)

$$\frac{dv}{dt} = -\frac{4}{3}\frac{x_e \sigma_T U_{cmb}}{m_p c} v = -\beta v,$$

where x_e is the electron fraction, σ_T is the Thompson cross section to electron scattering and $U_{cmb} = aT_{cmb}^4$ is the CMB energy density. By expressing the CMB temperature as a function of the redshift, z, we have $\beta = 2.06 \times 10^{-23} x_e (1+z)^4$ s^{-1}. Note that the typical time scale for Compton drag is $m_p/m_e \sim 1000$ times longer than the timescale for Compton cooling/heating.

The "Bondi" problem is described by the stationary equations of mass and momentum conservation (including the pressure, gravitational potential and viscosity term) and the equation of state of the gas. In spherical coordinates the equations are:

$$\begin{cases} \dot{M}_g & = 4\pi r^2 \rho v, \\ v\frac{dv}{dr} & = -\frac{1}{\rho}\frac{dP}{dr} - \frac{GM(<r)}{r^2} - \beta(z) v, \\ P & = K\rho^\gamma. \end{cases} \tag{1}$$

Here, v, r and ρ are the velocity, distance from the center of the gravitational potential and gas density. The "dot" represents the time derivative, thus $\dot{M}$ is the mass accretion rate. The gas pressure, P is assumed to be a power law of the density with exponent $1 \leq \gamma \leq 5/3$. This equation, know as the polytropic equation of state, substitutes the energy conservation equation. The case $\gamma = 1$ corresponds to an isothermal system in which the cooling time is much shorter than the dynamical time and the opposite limit, an adiabatic system, is obtained for $\gamma = 5/3$.

So far we have neglected the cosmological terms due to the Hubble expansion and dark matter. Also, we have implicitly assumed that the redshift-dependent viscous term, $\beta(z)$, changes slowly with respect to the time scale necessary to achieve stationarity: $t_{cr} \ll t_H$, where t_{cr} is approximately the sound crossing time and t_H is the Hubble time. We will return to this point in the next section.

2.1. *Hubble expansion: transition to self-similar solutions*

In order to include the cosmological term due to the Hubble expansion we use the standard procedure of writing the hydrodynamic equations (1) in a comoving frame of reference. This is done by expressing the radial coordinate, r, and the radial velocity, v, in terms of the comoving radius, x, and peculiar velocity, v_p:

$$\begin{cases} r & = a(t)x, \\ v & = \frac{d}{dt}(ax) = Hr + v_p. \end{cases} \tag{2}$$

Here, $a(t)$ is the scale factor, $H = \dot{a}/a$ is the Hubble parameter and the peculiar velocity is defined as $v_p = a\dot{x}$. The stationary ($\partial\delta/\partial t = 0$, $\partial v_p/\partial t = 0$) equations for the overdensity, $\delta = \rho/\overline{\rho}$, and peculiar velocity, v_p, are

$$\begin{cases} \dot{M}_p & = 4\pi x^2 (1+\delta) v_p, \\ \frac{v_p}{a}\frac{\partial v_p}{\partial x} & = -\frac{1}{\rho}\frac{dP}{adx} - \frac{G[\Delta M(<ax)]}{(ax)^2} - (\beta + H)v_p \end{cases} \tag{3}$$

Multiplying both sides of the mass conservation equation (top equation in [3]) by $\overline{\rho}(t)a(t)^2$, we recover the same equation as in (1), where $\dot{M}_g = \overline{\rho}(t)a(t)^2\dot{M}_p$ is now a function of time (or redshift). We also notice that $\partial/\partial r = a^{-1}\partial/\partial x$ and that $\Delta M(<r) = M(<r) - 4\pi\overline{\rho}r^3/3 \approx M(<r)$. Thus, neglecting the *self-gravity of the accreted gas*, the momentum conservation equation (the bottom equation in [3]) has the same form as in (1) after replacing β with the effective viscosity $\beta^{eff} = (\beta + H)$:

$$\begin{cases} \dot{M}_g & = 4\pi r^2 \rho(z) v_s, \\ v_s\frac{dv_s}{dr} & = -\frac{1}{\rho}\frac{dP}{dr} - \frac{GM(<r)}{r^2} - \beta^{eff}(z) v_s, \\ P & = K\rho^\gamma. \end{cases} \tag{4}$$

If we neglect the gas self-gravity, the cosmological expansion does not change the basic form of the equations but introduces: (i) an additional viscosity term in the momentum equation and (ii) the boundary conditions at $r \to \infty$ for the density $\rho_\infty(z)$ and the sound speed $c_{s,\infty}(z)$ are a function of redshift. Although we are assuming stationarity in the comoving frame of reference, the flow is time-dependent in physical coordinates. The assumption of steady flow is justified as long as the time scale to achieve the stationary solution in the comoving frame of reference is shorter than the Hubble time. We have already made this assumption when we have considered the Compton viscosity, $\beta(z)$.

2.1.1. *Stationarity*

The typical scale of the system is the Bondi radius r_b, hence, the sound crossing time is $t_{cr} \sim r_b/c_{s,\infty}$. If $t_{cr} < t_H$ the Bondi solution is valid because the cosmological terms vary slowly with respect to the typical time scale of the system and a quasi-steady solution can be found.

The analysis of the dimensionless accretion equations (see § 3) show that the viscosity term due to the Hubble expansion becomes important when $Hr_b/c_{s,\infty} > 1$. This condition is equivalent to the constrain $t_{cr} > t_H$. Thus, the assumption of stationarity, implicit in the derivation of the Bondi solution, fails when the Hubble term becomes important. In § 5, assuming a static PBH and neglecting feedback effects, we estimate that the hypothesis of stationarity fails for PBH masses $M_{PBH} \gtrsim 2 \times 10^4$ M$_\odot$. This is a conservative estimate because if we consider the proper motion of PBHs and feedback effects we derive a larger critical mass. However, the existence of PBHs more massive than $10^4 - 10^5$ M$_\odot$ is unlikely, so the cases for which the Bondi solution does not apply are not particularly relevant for the aim of the present study.

2.1.2. *Gas Self-gravity*

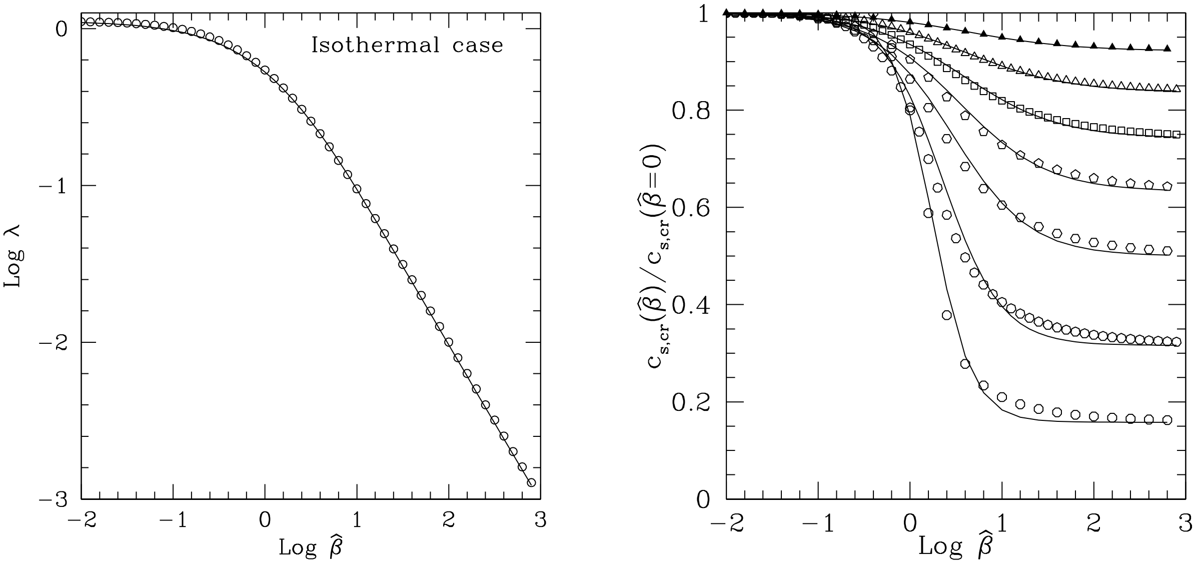

FIG. 1.— (*Left*). Dimensionless accretion rate λ onto a point mass as a function of the effective viscosity, $\hat\beta$, produced by Compton drag and Hubble expansion. We assume an isothermal equation of state for the gas. The points show the result of numerical integration and the curve shows the fit with the relationship in equation (9). (*Right*). The same as in the left panel but assuming a polytropic equation of state for the gas with $1 < \gamma \leq 5/3$. Instead of the accretion eigenvalue λ, here we show the sound speed at the sonic radius, $c_{s,cr}$ (normalized to its value neglecting viscosity, $\hat\beta = 0$), as a function of the effective viscosity $\hat\beta$. The accretion rate can be calculated from equation (8). The curves from top to bottom refer to $\gamma = 1.1, 1.2, 1.3, 1.4, 1.5, 1.6$ and 1.65, respectively.

The assumption of neglecting the self-gravity of the gas is justified if $M \gg M_{gas}$, where M_{gas} is the total gas mass contained in the halo around the black hole. It is easy to estimate the gas mass, M^B_{gas}, in the limit in which the viscosity terms are negligible (*i.e.*, for the classic "Bondi" solution). This estimate is a lower limit for M because $M \gg M^B_{gas} > M_{gas}$. By integrating the density profile for the Bondi solution we find that $M^B_{gas} \sim 8\pi/3\rho_\infty r_b^3$, where $r_b = GM/c^2_{s,\infty}$ is the Bondi radius. Thus, for $M \ll M^{cr} = (8\pi G^3/3)^{-1/2} c^3_{s,\infty}\rho_\infty^{-1/2}$ we can neglect the gas self-gravity. In the case of PBHs accreting from the IGM between the redshift of recombination and decoupling ($100 \lesssim z \lesssim 1000$) we have $c_{s,\infty} \approx 5.74$km s$^{-1}[(1+z)/1000]^{1/2}$ and $\rho_\infty = \rho_{cr}\Omega_b(1+z)^3$. Assuming $\Omega_b h^2 = 0.02$ we find $M^{cr} \sim 3 \times 10^5$ M$_\odot$. At later times ($30 \lesssim z \lesssim 100$) the critical PBH mass may become larger than M^{cr} because the temperature of the IGM may increase due to the radiation emitted by the gas accreting on the PBHs. The condition for steady accretion is more restrictive than the one found here. Thus, if steady solutions exist, the gas self-gravity can always be neglected.

The solution of the Bondi problem including the gas self-gravity has been studied in the context of stellar structure. The solution is known to be unstable for $\gamma < 4/3$. In this limit we would find that all the gas in the universe is eventually accreted onto PBHs. In the regime discussed here only a small fraction of the cosmic gas is accreted.

2.1.3. *Dark matter self-gravity*

The assumption of neglecting self-gravity of the accreting material is a good approximation for the baryons but not for the collisionless dark matter component. Unless all dark matter is constituted of primordial black holes (*i.e.*, $\Omega_{dm} = \Omega_{bh}$) we need to take into account the growth of structures seeded by the presence of PBHs (Mack et al. 2006). The total energy of a representative patch of the Universe at critical density is zero. Thus, the volume is marginally stable and the introduction of any perturbation, such as a PBH, produces the collapse of the region.

Mack et al. (2006) found that a dark matter halo about 100 times more massive than the primordial black hole at its center is accreted by redshift $z \sim 30$. The accretion takes place mostly after the epoch of "matter-radiation" equivalence. Calculations of the gas accretion rate into the gravitational potential produced by the dark matter halo will be considered in § 4. When a dark halo grows, the gas self-gravity can be neglected with respect to the dark matter potential because the total gas mass is about five times smaller (*i.e.*, the cosmic value) than the dark matter.

3. SPHERICAL ACCRETION ONTO A POINT MASS

3.1. *Sonic point*

It is convenient to write equation (4) in dimensionless units, $x = r/r_b$, $\mathcal{M} = v_s/c_s$, $\hat c_s = c_s/c_{s,\infty}$, $\hat\rho = \rho/\rho_\infty$, where $c_{s,\infty}$ and ρ_∞ are the sound speed and gas density at radii $r \to \infty$, respectively. The scaling constant for the radius, viscosity and accretion rate are:

$$r_b = \frac{GM_{bh}}{c^2_{s,\infty}}, \quad \hat\beta = \beta^{eff}\frac{r_b}{c_{s,\infty}} \quad \lambda = \frac{\dot M_g}{4\pi r_b^2 \rho_\infty c_{s,\infty}}. \tag{5}$$

We obtain the familiar set of dimensionless equations:

$$\begin{cases} \lambda &= \hat\rho^{\frac{\gamma+1}{2}}\mathcal{M}x^2 \\ \frac{\dot{\mathcal{M}}}{\mathcal{M}} &= \frac{\frac{2}{x}\left(1+\frac{(\gamma-1)}{2}\mathcal{M}^2\right)-\frac{\gamma+1}{2}\left(\frac{1}{\hat c_s^2 x^2}+\frac{\hat\beta\mathcal{M}}{\hat c_s}\right)}{\mathcal{M}^2-1} \\ \hat c_s &= \hat\rho^{\frac{\gamma-1}{2}} \end{cases} \tag{6}$$

The transonic solution crosses the sonic point ($\mathcal{M} = -1$) at the critical radius:

$$x_{cr} = \hat{c}_{s,cr}^{-2} \frac{-1 + \sqrt{1 + \hat{\beta}\hat{c}_{s,cr}^{-3}}}{\hat{\beta}\hat{c}_{s,cr}^{-3}}, \tag{7}$$

where $\hat{c}_{s,cr}$ is the dimensionless sound speed at the critical radius. In the limit of small effective viscosity (*i.e.*, $\hat{\beta}\hat{\ll}c^{3}_{s,cr}$) we find $x_{cr} \to (2\hat{c}^{2}_{s,cr})^{-1}$. In the limit of large effective viscosity we find $x_{cr} \to (\hat{c}_{s,c}\hat{\beta})^{-1/2}$. The eigenvalue, λ, for the transonic solution is

$$\lambda = \hat{\rho}_{cr}^{\frac{\gamma+1}{2}} x_{cr}^{2} = \hat{c}_{s,cr}^{\frac{\gamma+1}{\gamma-1}} x_{cr}^{2} \tag{8}$$

where $\hat{\rho}_{cr}$ is the dimensionless density at the critical radius.

3.2. *Accretion eigenvalues*

3.2.1. *Isothermal equation of state*

Since we did not find analytic solutions for equation (6), we integrated the equations numerically. We found the asymptotic solutions of the equations in the limits of negligible viscosity, $\hat{\beta} \to 0$, and large viscosity, $\hat{\beta} \to \infty$. In the limit of small viscosity we find the classic Bondi solution $\lambda \to \exp(3/2)x_{cr}^{2}$, where $x_{cr} = 0.5$. In the limit of large effective viscosity, the asymptotic analysis of equation (6) shows that $\hat{\rho}_{cr} \to 1$ and that $\lambda \to \hat{\beta}^{-1}$. We have used the asymptotic solutions for λ to guess the form of the appropriate fitting function of the numerical results. The function

$$\lambda = \exp\left[\frac{9/2}{3 + \hat{\beta}^{\,0.75}}\right] x_{cr}^{2}, \tag{9}$$

gives a good fit for the numerical results as shown in Fig. 1(left).

3.2.2. *Polytropic equation of state*

The asymptotic solutions for the cases of negligible effective viscosity and large effective viscosity can easily be found. Neglecting the viscosity terms we have $\hat{c}_{s,cr} \to [2/(5-3\gamma)]^{1/2}$. In the limit of large viscosity the asymptotic analysis of equation (6) shows that $\hat{\rho}_{cr} \to 1$, $\hat{c}_{s,cr} \to 1$ and $\lambda \to \hat{\beta}^{-1}$. We solve equation (6) numerically and find a parametric fit for the numerical results, with the correct asymptotic behavior for the sound speed at the critical radius. We also make sure that in the limit $\gamma \to 1$, the parametric fit for $\hat{c}_{s,cr}$ and λ have the same expression as that found for the isothermal case. We find

$$\hat{c}_{s,cr}(\hat{\beta}) = \frac{3\hat{c}_{s,cr}(0) + \hat{\beta}^{\xi}}{3 + \hat{\beta}^{\xi}},$$

$$\xi = 0.75 \left(\frac{\gamma+1}{5-3\gamma}\right)^{\frac{\gamma-1}{\gamma+1}}, \tag{10}$$

where $\hat{c}_{s,cr}(0) = [2/(5-3\gamma)]^{1/2}$ is the sound speed at the critical radius for $\hat{\beta} = 0$. The fitting curves (solid lines) and the numerical integrations (shown by the symbols) are shown in Fig. 1(right). The eigenvalue λ can be calculated for any given value of the polytropic index, γ, combining equations (8) and (10).

4. SPHERICAL ACCRETION INTO A DARK MATTER HALO

If dark matter is entirely composed of PBHs each of them would only accrete gas. In all the other cases a dark halo of WIMPs forms around each PBH. In this section we examine the gas accretion rate into the gravitational potential of a spherical dark matter halo with power-law density profile. The assumption of a single power-law for the density profile is partially dictated by the need for simplicity but it is also justified theoretically as elucidated below.

PBHs accumulate a spherical halo of dark matter that grows in mass proportionally to $(1+z)^{-1}$. Non-negligible growth of the dark matter halo begins at matter-radiation equality, and by redshift $z \simeq 30$ the black hole is embedded in a halo about 100 times its original mass (Mack et al. 2006). The numerical values of the halo mass and the comoving turnaround radius are:

$$M_h = 3M_{PBH}\left(\frac{1+z}{1000}\right)^{-1}, \tag{11}$$

$$r_{ta,com} = 58\ \text{pc}\left(\frac{M_h}{1\ M_\odot}\right)^{1/3}. \tag{12}$$

The theory of secondary infall predicts that the dark halo has a radial density profile that is well approximated by a single power-law cusp and a truncation of the density profile at a fraction of the turnaround radius. All of the halo mass is contained within the cusp. Two types of time-dependent, self-similar solutions have been found for the dark matter profile (Gunn & Gott 1972; Fillmore & Goldreich 1984; Bertschinger 1985); the transition from one type to the other depends on the amount of angular momentum of the infalling matter:

a) If the flow is highly radial such that the PBH at the center absorbs all of the infalling matter, then almost all the mass in the accreting halo is eventually incorporated into the central black hole. This infall solution is characterized by the free-fall boundary condition at the center and pressureless matter at infinity. The solution is also valid for "cold" gas accretion because there is no shell crossing and no standing shock forms. The self-similarity of the solution is valid if $M_h > M_{PBH}$, when the matter is self-gravitating. Near the center the halo mass is negligible compared to the black hole mass, so the matter is free falling and the density profile is $\rho \propto r^{-3/2}$. This slope is the same as for the Bondi solution inside the sonic radius. In the outer parts the solution is very different from the Bondi solution. The radial density profile, due to the Hubble expansion, decreases with radius propotionally to r^{-3}. The radius r_h of the "free-fall" cusp depends on the details of the collapse but is typically $r_h/r_{ta} \ll 1$ (Mack et al. 2006).

b) If the flow is quasi spherical but the angular momentum of the accreting dark matter prevents direct accretion onto the central black hole, the particles pass near the center without being absorbed. For the case in which the accreting matter is collisional, a standing shock inside the turnaround radius stops the gas infall within the core. Remarkably, the solution for collisionless matter is very similar to the $\gamma = 5/3$ solution for gas accretion. The density profile has slope $\alpha = 2.25$ at $r < r_h = 0.339 r_{ta}$. For $r > r_h$ the overdensity is close to one.

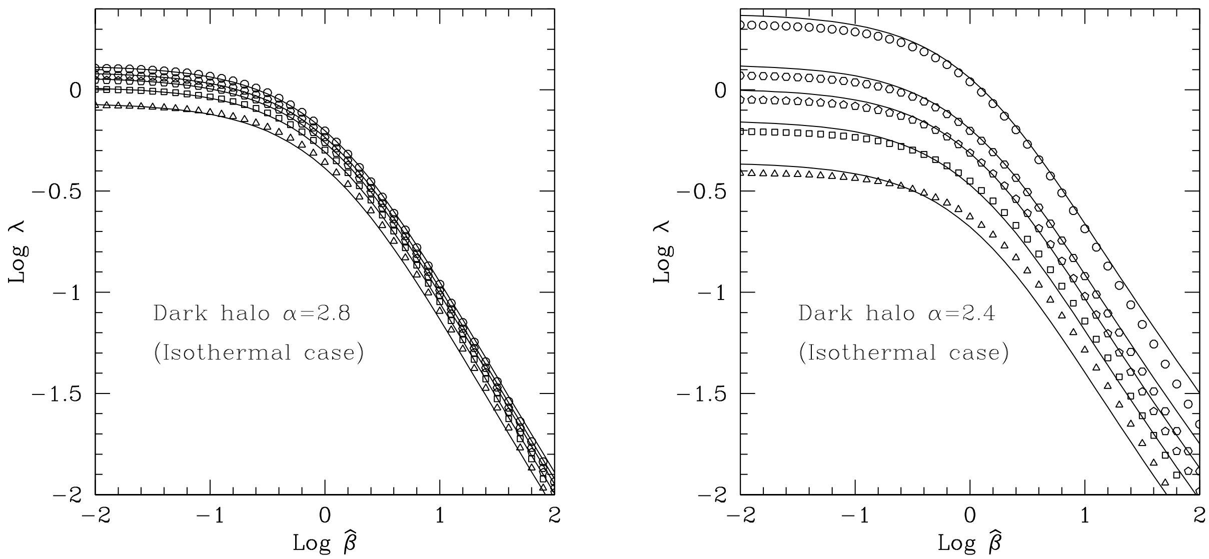

FIG. 2.— (*Left*). Dimensionless accretion rate λ into a spherical dark matter halo as a function of the effective viscosity, $\hat{\beta}$, produced by Compton drag and Hubble expansion. Each curve, from bottom to top, refers to halos of increasing radius. If the radius of the halo is smaller than the accretion radius, r_B, defined in the text, the accretion rate into an extended halo equals the one calculated for a point mass. We assume isothermal equation of state for the gas and a power-law density profile of the dark halo with slope $\alpha = 2.8$. From bottom to top the symbols show the result of numerical integration and the curves show the fits with the parametric relationship in equation (18) for values of the dimensionless halo radius $r_B/r_h = \chi^{1/(1-p)} = 2, 1, 0.5, 0.25$ and 0.016. (*Right*). The same but for $\alpha = 2.4$.

Estimates of the angular momentum of the accreting dark matter onto PBHs are presented in a companion paper (Ricotti et al. 2006). Based on the results of the angular momentum calculations case (b) is the most relevant. Nevertheless, if a fraction of the dark matter is captured by the central PBH, we expect that the density profile has properties intermediate between case (a) and (b). The truncation radius r_h would be smaller than $r_{ta}/3$, and the effective slope of the inner density profile steeper than 2.25, in order to take into account the non-negligible mass of the central black hole. Indeed a halo with slope of the density profile $\alpha = 3$ has a potential that approaches the one of a point mass with $M \sim M_h$. For the sake of generality we take this effects into account by treating the core radius r_h and slope of the core density profile as free parameters.

We calculate of the gas accretion rate by replacing the gravitational acceleration for a point mass ($g_{bh} = -GM_{bh}/r^2$) in equation (6) with that for an extended dark halo with power-law density profile: $\rho = \Delta\rho_{dm}(z)[r/r_h]^{-\alpha}$. Here, $\rho_{dm}(z)$ is the mean dark matter density at redshift z and Δ is the overdensity of the halo at $r = r_h$. We assume that all the mass of the halo is within the radius r_h. Thus, the gravitational acceleration is

$$g_{dm}(r) = -\frac{GM_h}{r^2}\min[(r/r_h)^p, 1], \qquad (13)$$

where $p = 3 - \alpha$. Note that the halo radius is smaller than the turnaround radius: $r_h < r_{ta}$. We explore the range of values $2 < \alpha < 3$ for the log-slope of the density profile (*i.e.*, $0 < p < 1$). If $p \to 0$ the gravitational acceleration approaches the point-mass value. If the halo radius is $r_h \leq x_{cr} = 0.5 r_b = 0.5 GM_h/c_{s,\infty}^2$, the accretion eigenvalue is given by equation (9), the same as replacing the halo with a point-mass $M = M_h$. Thus, it is apparent that the accretion rate onto an extended halo is a function of the dimensionless parameter $\chi = r_b/r_h$ and the parameter p. The case $p = 1$ describes the density profile for an isothermal sphere for which the circular velocity is a constant. This case is singular because the Bondi radius, for which $v_{cir}(r_b) = c_s$, cannot be defined.

4.1. *Sonic point*

After substituting $g(r)$ in equation (4) with the expression given in equation (13) for $g_{dm}(r)$, we rewrite the equations in dimensionless units, $x = r/r_B$, $\mathcal{M} = v_s/c_s$, $\hat{c}_s = c_s/c_{s,\infty}$, $\hat{\rho} = \rho/\rho_\infty$, where $c_{s,\infty}$ and ρ_∞ are the sound speed and gas density respectively, at radii $r \to \infty$. Note that the scale radius, r_B, for spherical accretion onto an extended halo of mass M_h is not defined analogously to point-mass Bondi radius, $r_b = GM_h/c_{s,\infty}^2$, of equivalent total mass. It is convenient to express the dimensional constants for an extended halo as a function of the parameter $\chi = r_b/r_h$:

$$r_B = r_h \chi^{\frac{1}{1-p}} = r_b \chi^{\frac{p}{1-p}} \qquad (14)$$

where $1 \leq (1-p)^{-1} \leq \infty$ and $0 \leq p/(1-p) \leq \infty$ for $2 < \alpha < 3$. The dimensionless viscosity and accretion rate are defined as:

$$\hat{\beta} = \beta^{eff}\frac{r_b}{c_{s,\infty}}\chi^{\frac{p}{1-p}}, \quad \lambda = \frac{\dot{M}_g}{4\pi r_b^2 \rho_\infty c_{s,\infty}}\chi^{-\frac{2p}{1-p}}. \qquad (15)$$

In these units we obtain the dimensionless equation:

$$\frac{\dot{\mathcal{M}}}{\mathcal{M}} = \frac{\frac{2}{x}(1 + \frac{(\gamma-1)}{2}\mathcal{M}^2) - \frac{\gamma+1}{2}\left(\frac{1}{\hat{c}_s^2 x^{2-p}} + \frac{\hat{\beta}\mathcal{M}}{\hat{c}_s}\right)}{\mathcal{M}^2 - 1}. \qquad (16)$$

The transonic solution crosses the sonic point ($\mathcal{M} = -1$) at the critical radius $x_{cr,dm}$, found by solving the equation

$$\hat{\beta}\hat{c}_{s,cr} x_{cr,dm}^{2-p} + 2\hat{c}_{s,cr}^2 x_{cr,dm}^{1-p} - 1 = 0, \qquad (17)$$

where $\hat{c}_{s,cr}$ is the dimensionless sound speed at the critical radius. It is useful to find the asymptotic behaviors of the critical radius in the limit of zero viscosity,

$x_{cr,dm} \to (2\hat{c}^2_{s,cr})^{-1/(1-p)}$ and in the limit of large viscosity $x_{cr,dm} \to (\hat{c}_{s,cr}\hat{\beta})^{-1/(2-p)}$. These asymptotic behaviors will guide us to find the functional form of the fitting formula.

4.2. *Accretion eigenvalues*

For the sake of simplicity, given that we have introduced two new free parameters that describe the halo potential, we will only discuss the case of an isothermal equation of state for the gas. Physically, the isothermal equation of state is the most relevant case because the CMB photons that exert Compton drag are about 1000 times more efficient in keeping the gas temperature constant, and close to the CMB value.

4.2.1. *Isothermal equation of state*

The accretion eigenvalue can be fitted with the following approximate formula

$$\lambda^h = f_\beta f_\chi \exp\left[\frac{9/2}{3+\hat{\beta}^{\,0.75}}\right] x^2_{cr,dm}, \tag{18}$$

where the functions

$$f_\beta = 1 + 1.25\hat{\beta}^{\frac{p}{2-p}}, \tag{19}$$

$$f_\chi = \left[\exp(2-\chi)\right]^{\frac{p}{1-p}}, \tag{20}$$

are small corrections to λ that vanish for small values of p and $\chi \to 2$. This formula cannot be used without an expression for $x_{cr,dm}$. The function f_β has been derived from the asymptotic analysis of the equation for the critical radius $x_{cr,dm}$. Assuming an isothermal equation of state, the sonic radius approaches $x_{cr,dm} \to 2^{-1/(1-p)}$ in the limit of negligible effective viscosity, and $x_{cr,dm} \to \hat{\beta}^{-1/(2-p)}$ in the limit of large effective viscosity. Thus, the sonic radius of the transonic solution for accretion into a halo potential is related to that of a point-mass (with $M = M_h$) by the approximate fitting formula

$$\frac{x_{cr,dm}}{x_{cr}} \approx 2^{-\frac{p}{1-p}} \left(\frac{g_\beta}{f_\beta}\right)^{1/2}, \tag{21}$$

where

$$g_\beta = \left(1 + 10\hat{\beta}\right)^{\frac{p}{10(1-p)}}. \tag{22}$$

Combining equations (21) and (18) we can relate the accretion eigenvalue for an extended dark matter halo to the eigenvalue in equation (9) for a point mass $M = M_h$:

$$\frac{\lambda^h}{\lambda^{bh}} = 2^{\frac{2p}{1-p}} g_\beta f_\chi. \tag{23}$$

The fits using the parametric function equation (18) to the numerical integrations are shown in Fig. 2 for different values of α and the parameter χ.

It is important to note that the dimensional units for the accretion rate, radius and effective viscosity are different for the cases of a dark matter potential and a point-mass. Thus the dimensional accretion rate into a halo is reduced by a factor $\chi^{2p/(1-p)}$ and the effective viscosity increases by a factor $\chi^{p/(1-p)}$ with respect to the point-mass case. To summarize, the accretion rate into a halo of mass M_h is related to the accretion rate onto a black hole of equivalent mass M_{bh} by the relationship

$$\hat{\beta}^h \equiv \chi^{\frac{p}{1-p}} \hat{\beta}^{bh}, \tag{24}$$

$$\lambda^h \equiv \Upsilon^{\frac{p}{1-p}} \lambda^{bh}, \tag{25}$$

$$r^h_{cr} \equiv x_{cr,dm} r_B = \left(\frac{g_\beta}{f_\beta}\right)^{1/2} \left(\frac{\chi}{2}\right)^{\frac{p}{1-p}} r_{cr}, \tag{26}$$

where

$$\Upsilon = \left(1 + 10\hat{\beta}^h\right)^{\frac{1}{10}} \exp\left(2-\chi\right) \left(\frac{\chi}{2}\right)^2. \tag{27}$$

Note that $\hat{\beta}^h$ and not $\hat{\beta}^{bh}$ should be used in the analytic expressions for λ^{bh} and r_{cr}.

5. SUMMARY AND DISCUSSION

This paper examines the classic Bondi problem of steady, spherical gas accretion in a cosmological framework. The main motivation of the present work is to determine the accretion rate onto primordial black holes in the early universe, before the formation of the first galaxies and stars. We estimate the importance of cosmological effects such as the gas viscosity due to the coupling of the gas to the CMB photon fluid (Compton drag), the Hubble expansion and the formation of a dark halo around the black hole. In a companion paper we use the results of the present work to model cosmic ionization by the X-rays emitted from accreting PBHs. Comparisons between theoretical models and WMAP3 data allow us to constrain mass and abundances of PBHs (Ricotti et al. 2006).

The cosmological Bondi problem is tightly related to the theory of "secondary infall" developed by Gunn & Gott (1972); Fillmore & Goldreich (1984); Bertschinger (1985). In the standard cosmological model the baryons are a small fraction of the dark matter, hence the evolution of dark matter is unaffected by the presence of the gas. We use the results of the secondary infall theory to determine the shape of the gravitational potential into which the gas is infalling. In addition, when the viscosity term due to cosmic expansion becomes important, the assumption of steady flow for the gas, implicit in deriving the Bondi solution, becomes invalid. In this limit, time-dependent infall solutions should be used instead. In § 5.3 we discuss the relationships between the Bondi and the secondary infall solutions and the conditions of validity for each of them.

5.1. *Accretion onto a point mass*

The physical values for the accretion rate and the critical radius are easily calculated from the dimensionless ones. The values of the Bondi-Hoyle radius, r_b, and accretion rate are

$$r_b \approx 43.3 \text{ pc} \left(\frac{M}{10^4 M_\odot}\right) \left(\frac{c_{s,\infty}}{1\text{km s}^{-1}}\right)^{-2}, \tag{28}$$

$$\dot{M} \approx \lambda(3.7 \times 10^{22} \text{ g s}^{-1}) n_{\rm gas} \left(\frac{M}{10^4 M_\odot}\right)^2 \left(\frac{c_{s,\infty}}{1\text{km s}^{-1}}\right)^{-3} \tag{29}$$

respectively (Bondi & Hoyle 1944). The accretion rate eigenvalue, λ, is a function of the dimensionless "effective viscosity", $\hat{\beta} = \beta^{eff} t_{cr}$, where the Bondi radius crossing time is $t_{cr} = r_b/c_{s,\infty}$ and $\beta^{eff} = \beta(z) + H(z)$. In the

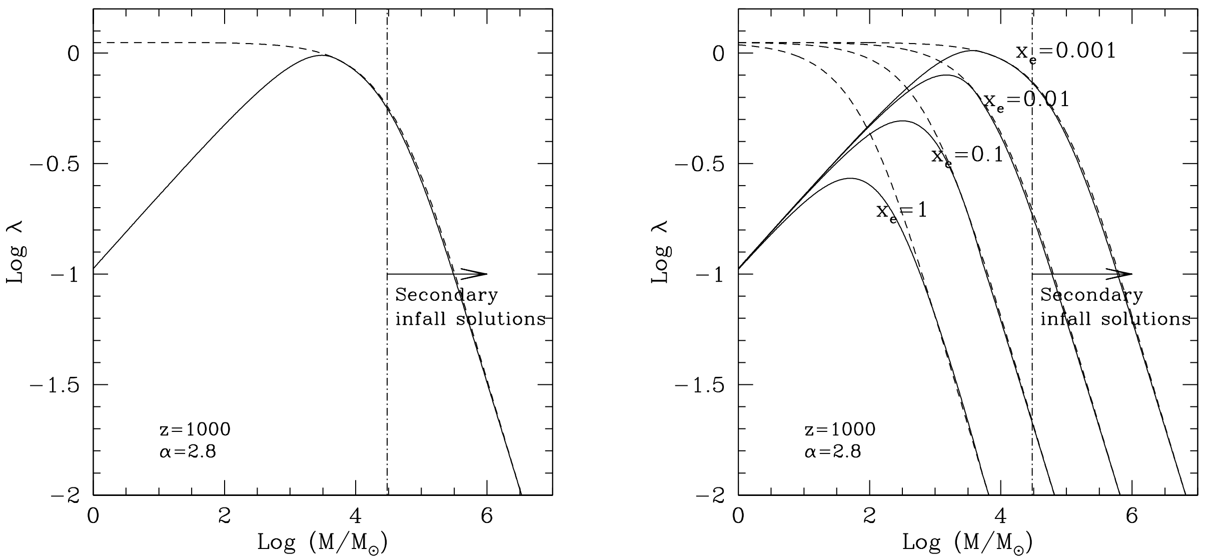

FIG. 3.— (*Left*). Dimensionless accretion rate λ into a spherical dark matter halo (solid curve) and a point mass (dashed curve) as a function of the mass of the object (PBH or dark halo) at $z + 1 = 1000$. We have considered only the viscosity from the Hubble expansion and a halo with power-law slope $\alpha = 2.8$. (*Right*). The same as the left panel but considering only the viscosity due to Compton drag. The different curves refer to gas with fractional ionization $x_e = 1, 0.1, 0.01$ and 0.001 as shown by the labels.

relevant redshift range (*i.e.*, before $z \sim 30$) the Compton drag term is $\beta(z) \propto x_e(1+z)^4$ and the Hubble parameter is $H(z) = 3.24 \times 10^{-18} s^{-1} (\Omega_m h^2)^{1/2} (1+z)^{3/2}$. It follows, assuming $\Omega_m h^2 = 0.127$ (Spergel et al. 2006), that $\beta^{eff} = H(z)\{1 + 1.78 x_e[(1+z)/100]^{5/2}\}$ and the Compton term is dominant over the Hubble term at redshifts

$$z > 500 \left(\frac{x_e}{0.01}\right)^{-2/5}. \tag{30}$$

The gas viscosity can be neglected if $\beta^{eff} t_{cr} < 1$, where

$$t_{cr} = \frac{r_b}{c_{s,\infty}} = (0.224\,\mathrm{Myr}) \left(\frac{M}{10^4\ M_\odot}\right) \left(\frac{c_{s,\infty}}{5.74\ \mathrm{km\ s^{-1}}}\right)^{-3}.$$

Including the Hubble flow and Compton drag terms, the expression for the dimensionless effective viscosity is

$$\hat{\beta} = \left(\tfrac{M}{10^4 M_\odot}\right) \left(\tfrac{z+1}{1000}\right)^{3/2} \left(\tfrac{c_{s,\infty}}{5.74\mathrm{kms^{-1}}}\right)^{-3} \times \left[0.257 + 1.45 \left(\tfrac{x_e}{0.01}\right) \left(\tfrac{z+1}{1000}\right)^{5/2}\right]. \tag{31}$$

Let us consider first the viscosity term due to the Hubble expansion. We can neglect the Hubble flow when $t_{cr} < t_H = H(z)^{-1}$ or, equivalently, when $v_H/c_{s,\infty} < 1$, where $v_H = r_b H(z)$ is the typical Hubble velocity of the gas at the Bondi radius. If we assume that the gas temperature equals the CMB temperature, $c_{s,\infty} = 1.1$ km/s$(T_{cmb}/100K)^{1/2}$, we find that $t_{cr} < t_H$ for

$$M_{pbh} < 2.7 \times 10^4\ \mathrm{M_\odot}. \tag{32}$$

Hence, the accretion onto primordial black holes less massive than 3×10^4 M$_\odot$ (or more massive if the gas temperature is $T_{gas} > T_{cmb}$ due to photo-heating from accreting PBHs) is weakly affected by the Hubble expansion. But, as discussed in detail in § 5.3, when the Hubble viscosity becomes important the hypothesis of quasi-steady flow fails and the Bondi solution transitions to the time-dependent secondary infall solution.

Assuming that the gas temperature equals the CMB temperature, the viscosity term due to Compton drag is negligible for

$$M_{pbh} \lesssim \frac{70\ \mathrm{M_\odot}}{x_e} \left(\frac{z+1}{1000}\right)^{-5/2}.$$

Before recombination, PBHs with mass $M_{pbh} \lesssim 50 - 100$ M$_\odot$ are unaffected by Compton drag. Instead, the accretion rate onto PBHs more massive than $100 - 1000$ M$_\odot$ is negligible before recombination. In the standard cosmological model the residual ionization fraction after recombination is $x_e \sim 10^{-4}$, hence, after recombination, Compton drag is negligible for any reasonable PBH mass. Only if a sufficiently large number of PBHs or other sources of ionizing radiation increase the fractional ionization above $x_e \gtrsim 1.47 \times 10^{-3}$ the Compton viscosity becomes important (*i.e.*, dominant with respect to the viscosity term due to the Hubble flow).

The eigenvalue λ can be derived from the equation of mass conservation (8) that depends on the polytropic index, γ, the sonic point, $x_{\rm cr}$ [given by equation (7)], and the sound speed at the sonic point, $c_{\rm s,cr}$. We provide fits to the sound speed at the sonic point (see Fig. 1) in equation (10). In the limit $\gamma = 1$ (isothermal equation of state) the accretion eigenvalue is given by equation (9) and depends only on $x_{\rm cr}$.

5.2. *Accretion into a dark matter halo*

If the radius of the dark matter halo, r_h, is within the Bondi critical radius, the accretion rate is unchanged with respect to the case of a point mass. Quantitatively, the accretion rate is reduced approximately by $(\chi/2)^{2p/(1-p)}$ with respect to the point mass case where

$$\frac{\chi}{2} = \frac{r_b}{2r_h} = 3.3{\times}10^{-3} \left(\frac{M_h}{1M_\odot}\right)^{\frac{2}{3}} \left(\frac{1+z}{1000}\right) \left(\frac{c_{s,\infty}}{5.74\mathrm{kms^{-1}}}\right)^{-2}. \tag{33}$$

If $\chi/2 \geq 1$ the extended dark halo accretes as a point-mass with $M = M_h$. Assuming $T_{gas} = T_{cmb}$, which is a good approximation for $z > z_{dec} \sim 100$, we have approximately

$$\frac{\chi}{2} \approx \left(\frac{M_h}{M_h^{cr}}\right)^{\frac{2}{3}},$$

where $M_h^{cr} = 5196$ M$_\odot$.

In Fig. 3 we compare the dimensionless accretion rate at $z = 1000$ for a point mass (dashed curves) and an extended halo (solid curves) as a function of their mass. The left panel shows the case in which the effective gas viscosity is dominated by the Hubble flow and the right panel shows the opposite case in which Compton drag dominates. The results for an extended dark halo shows that the accretion rate peaks at $M \sim M_h^{cr}$. This can be easily understood due to two competing effects. The gas effective viscosity becomes larger with the increasing mass of the accreting object, thus the accretion eigenvalue λ is reduced as the mass increases. However, the accretion rate eigenvalue for an extended dark matter halo is increasingly reduced with respect to the point mass case as the halo mass decreases. If $M_h \gtrsim 10^4$ M$_\odot$ we have that $r_B > r_{ta}$. We will show in § 5.3 that in this regime the Bondi solution becomes invalid and the gas flow transitions to the time-dependent self-similar solution described by the theory of secondary infall.

The ratio between the accretion rate onto a PBH clothed with a dark halo and the same PBH without dark halo ("naked") is approximately

$$\frac{\dot{M}_h}{\dot{M}_{bh}} = \mathrm{Max}\left\{\left(\frac{M_{bh}}{M_h^{cr}}\right)^{\frac{4p}{3(1-p)}}\left[\frac{1}{\phi_i}\left(\frac{1+z}{1000}\right)\right]^{-\frac{(6-2p)}{3(1-p)}}, 1\right\},$$

and is very sensitive to the slope of the halo density profile. At a given redshift z, the effect of the halo growth becomes important in increasing the accretion rate if PBHs have a mass $M_{PBH} > M_h^{cr}[(z+1/1000)/\phi_i]^{(3-p)/2p}$. For example, assuming a steep dark matter density profile with $p = 0.2$, any PBH "clothed" in its dark halo, with a mass $M_{PBH} > 2.37$ M$_\odot[(3/\phi_i)(1+z)/1000]^7$ accretes significantly more and its accretion rate increases rapidly with time ($\propto (1+z)^{-7/3}$) with respect to a "naked" PBH of the same mass. As noted in § 4, density profiles steeper than $\alpha = 2.25$ may be used to describe a halo with $M_h \sim M_{pbh}$, in order to take into account the potential of the central PBH. Thus, at redshifts $z \lesssim 500$, when $M_h \gg M_{pbh}$, the fiducial value of the density profile slope is $\alpha = 2.25$ according to the secondary infall theory. In this case ($p = 0.75$ and $\phi_i = 3$) the effect of the dark matter halo becomes significant for relative massive PBHs: $M_{pbh} > 1000$ M$_\odot[(1+z)/1000]^{1.5}$, or $M_{pbh} \gtrsim 32$ M$_\odot$ at redshift $z \sim 100$.

5.3. *Transition to time-dependent secondary infall solutions*

The cosmological Bondi solution rests on the assumption of steady and non-self-gravitating spherical gas accretion. In comoving coordinates the gas is at rest at infinity with sound speed, $c_{s,\infty}$. Conversely, secondary infall solutions describe self-similar and time-dependent spherical accretion in an expanding universe. They depend on the assumption that the matter is self gravitating and its sound speed at infinity is $c_{s,\infty} \to 0$ ("cold" cosmological accretion). Thus, the regime of validity of secondary infall solutions is complementary to the Bondi solutions. The accretion is effectively "cold" if the sound speed at infinity is much smaller than the Hubble flow: $c_{s,\infty} \ll r_b H$. This condition is equivalent to $t_{cr} < t_H$; that is, when the hypothesis of quasi-steady flow fails for the Bondi problem. As shown in § 5.1, for an accreting point mass the transition from steady to self-similar solutions is for $M_{pbh} \gtrsim 2 \times 10^4$ M$_\odot$. This case is of little interest because the formation of PBHs with such a large mass is unlikely. Moreover, we show later that the accretion rate is super-Eddington, thus regulated by complex feedbacks, the modeling of which is beyond the scope of this paper.

When PBHs do not constitute the bulk of the dark matter a dark halo accumulates around them. Assuming, for simplicity, $T_{gas} = T_{cmb}$ we find that if $M_h \gtrsim 10^4$ M$_\odot$ the Bondi radius is larger than the dark matter turnaround radius: $r_B > r_{ta}$. This result is clearly incorrect because the gas cannot be accreted from radii larger than the dark matter turnaround radius and is simply a consequence of neglecting the Hubble expansion. This suggests that the Bondi solution fails in this regime and the gas flow becomes time-dependent. Indeed, when $r_B = GM_h/c_{s,\infty}^2 > r_{ta}$ the halo circular velocity is larger than the gas sound speed, $(GM_h/r_{ta})^{1/2} = v_{cir} > c_{s,\infty}$. Thus, the Bondi solutions transition to "cold" cosmological gas infall, for which self-similar solutions exist. In addition, since Hubble velocity at the turnaround radius equals the halo circular velocity, $r_{ta}H \sim v_{cir}$, we also have $t_H < r_{ta}/c_{s,\infty} < t_{cr}$. The assumption of steady flow is therefore no longer correct and the flow becomes self-similar and time-dependent.

Self-similar infall solutions for a mixture of gas and dark matter (assuming that the gas is a small fraction of the dark matter) are almost identical to the case of cold gas infall. The main difference is that well behaved solutions exist for $\gamma \leq 4/3$ because the gravitational instability, leading to collapse for $\gamma \leq 4/3$, occurs only if the gas is self-gravitating. Two types of self-similar solutions exist. If the central black hole absorbs all the infalling gas, the solution has free-fall boundary conditions at the center (see discussion in § 4). Most of the halo gas is accreted onto the central black hole, hence the accretion rate in units of the Eddington rate is $\dot{m} = \dot{M}/\dot{M}_{Ed} \sim t_{Ed}/t_H$. Since $t_{Ed} \sim 10^7$ yrs, $\dot{m} \gg 1$ at any redshift $z \gtrsim 30$. The second type of solution is characterized by shocked accretion of collisional gas. The boundary conditions are $v = 0$ at the center (*i.e.*, no accretion onto the central black hole) and pressureless gas upstream of the shock. A standing shock occurs at a fixed fraction of the turnaround radius r_s/r_{ta}, whose value depends on the polytropic index γ. For $\gamma = 5/3$ the shock is at $r_s = 0.339 r_{ta}$, analogous to the result for collisionless matter. For smaller values of γ the shocked core is smaller. Self-similar solutions can be found also for the cases in which the central black hole accretes an arbitrary fraction of the infalling gas. In this case the size of the shocked core is further reduced. Tsuribe et al. (1995) found a self-similar solution for spherical accretion around a point mass including radiation drag. They conclude that radiation drag (i) slows down the infalling gas velocity far from the center, (ii) flattens the density profile near the center, and (iii) reduces the mass-accretion rate. The reduction is about a factor of two if the gas becomes fully ionized by redshift $z \sim 400 - 200$.

Taking into account all the possible accretion regimes described above may be quite complex (Loeb 1993; Fukue & Umemura 1994; Mineshige et al. 1998; Ciotti et al. 2004; Wang et al. 2006; Park & Ostriker 2007). Fortunately, it is not necessary to estimate in detail the accretion rate for the cases in which the flow is time-dependent. This is because it is easy to show that the accretion rate is always greater than the Eddington rate. Feedback effects are likely to regulate the accretion rate in this regime. Observations of quasars at moderate redshifts and theoretical arguments (Ciotti & Ostriker 2001) suggest that when the gas supply is large ($\dot{m} > 0.1 - 1$), massive black holes shine at nearly the Eddington rate during a small fraction $\sim 1 - 5\%$ of their life, while during the rest of the time they are quiescent. Most of the energy is emitted during the active phases. Theoretical modeling of feedback processes that produce the duty cycle is beyond the scope of the present paper. We can treat this case phenomenologically assuming a fiducial value of the duty cycle inferred from observations.

In order to demonstrate that when $t_{cr} > t_H$ we have $\dot{m} \gg 1$, it is convenient to rewrite the Bondi accretion formula in equation (29), in terms of the crossing time and Hubble time. Using the relationship $t_H^{-2} = (\Omega_{dm}/\Omega_b) G\rho_{gas} \sim 5G\rho_{gas}$, and assuming $t_{cr} \gtrsim t_H$ and $\lambda \sim 1$, we have

$$\dot{m} \sim \lambda \frac{t_{Ed} t_{cr}}{5 t_H^2} \gtrsim \frac{t_{Ed}}{5 t_H} \gg 1,$$

at any redshift $z > 30$. Thus, as anticipated, when the accretion flow transitions to a time-dependent self-similar regime, the accretion rate is super-Eddington.

ACKNOWLEDGMENTS

Many thanks to Jerry Ostriker for suggesting ideas that motivated this paper and the anonymous referee for useful feedback.

REFERENCES

Alcock, C., et al. 2000, ApJ, 542, 281
Bertschinger, E. 1985, ApJS, 58, 39
Bondi, H., & Hoyle, F. 1944, MNRAS, 104, 273
Carr, B. J. 1981, MNRAS, 194, 639
Carr, B. J. 2003, LNP Vol. 631: Quantum Gravity: From Theory to Experimental Search, 631, 301
Carr, B. J., & Hawking, S. W. 1974, MNRAS, 168, 399
Ciotti, L., & Ostriker, J. P. 2001, ApJ, 551, 131
Ciotti, L., Ostriker, J. P., & Pellegrini, S. 2004, in AIP Conf. Proc. 703: Plasmas in the Laboratory and in the Universe: New Insights and New Challenges, ed. G. Bertin, D. Farina, & R. Pozzoli, 367
Fillmore, J. A., & Goldreich, P. 1984, ApJ, 281, 1
Fukue, J., & Umemura, M. 1994, PASJ, 46, 87
Gunn, J. E., & Gott, J. R. I. 1972, ApJ, 176, 1
Hamadache, C., et al. 2006, A&A, 454, 185
Harada, T., & Carr, B. J. 2005, Phys. Rev. D, 71, 104009
Hawking, S. 1971, MNRAS, 152, 75
Jedamzik, K. 1997, Phys. Rev. D, 55, 5871
Loeb, A. 1993, ApJ, 403, 542
Mack, K., Ostriker, J., & Ricotti, M. 2006, ApJ, in press, astro-ph/0608642
Miller, M. C., & Ostriker, E. C. 2001, ApJ, 561, 496
Mineshige, S., Tsuribe, T., & Umemura, M. 1998, PASJ, 50, 233
Musco, I., Miller, J. C., & Rezzolla, L. 2005, Classical and Quantum Gravity, 22, 1405
Park, M.-G., & Ostriker, J. P. 2007, ApJ, 655, 88
Peebles, P. J. E. 1980, The large-scale structure of the universe (Research supported by the National Science Foundation. Princeton, N.J., Princeton University Press, 1980. 435 p.)
Ricotti, M., Ostriker, J., & Mack, K. 2006, ApJ, submitted
Sasaki, S., & Umemura, M. 1996, ApJ, 462, 104
Spergel, D. N., et al. 2006, ArXiv Astrophysics e-prints
Tsuribe, T., Umemura, M., & Fukue, J. 1995, PASJ, 47, 73
Umemura, M., & Fukue, J. 1994, PASJ, 46, 567
Umemura, M., Loeb, A., & Turner, E. L. 1993, ApJ, 419, 459
Wang, J.-M., Chen, Y.-M., & Hu, C. 2006, ApJ, 637, L85